Monte Carlo Simulation of NUREG/CR 6850 Appendix L Model for Main Control Board Fires and Resulting Insights

Paul Boneham, Paul Guymer, Mike Wright
Jacobsen Analytics Ltd, Congleton, United Kingdom

Abstract: In the absence of an existing verified and validated computational tool to determine the probability of damage to a target set of components due to a Main Control Board (MCB) fire, a method was proposed in NUREG/CR-6850 Appendix L. This method has the advantage that it reduces analysis of a potentially large number of MCB fire scenarios to consideration of a limited number of individual target sets of critical MCB components/cables with each target set being defined only by a single parameter, the maximum separation distance (d) between them.

This paper describes a Monte-Carlo simulation of the Appendix L method and demonstrates its flexibility and ease of use to: a) address the updated cabinet heat release rate profiles and non-suppression probabilities proposed in NUREG-2178 and NUREG-2169 respectively, b) propose a practical solution for evaluating specific MCB configurations where ignition sources or cable raceways may be present in rear sections of the cabinet as identified in FPRA FAQ 14-008 and c) evaluate the benefit of solid metal partitions within the MCB in an integrated fashion. As part of this process, the Monte Carlo approach is benchmarked against NUREG/CR-6850 Appendix L and a related NEI Task Force White Paper which is currently undergoing review. The full paper presents some improvements to the NUREG/CR-6850 approach based on insights from the benchmarking exercise.

Keywords: Internal Fire PSA, Fire Modeling, Main Control Board, NUREG/CR 6850 Appendix L

1. INTRODUCTION

NUREG/CR 6850 (1), Appendix L (hereafter referred to as “Appendix L”) presents an analytical method for estimating the probability of fire damage to a target set of components on the front panel of a vertical Main Control Board. Results are presented in Appendix L for the specific case of a panel 60 ft.(18.29m) wide and 10 ft.(3.05m) high. For panels with different dimensions it would be necessary to repeat the analysis making the appropriate changes to the limits of integration. Moreover, to simplify the analysis, a number of assumptions and approximations were made that limit the applicability of the analytical method to practical situations. These assumptions are highlighted in a review of the Appendix L methodology, summarized below.

The limitations of the Appendix L methodology can be surmounted by using the Monte-Carlo simulation technique, which provides a powerful and flexible tool for solving a wide range of practical problems. The application of this technique and results using the physical model described in (1), Appendix L is described.

2. APPENDIX L FORMULATION

Physical Model

Appendix L considers a target set of two components mounted on the front panel of a vertical main control board a distance (d) apart (see Figure 1). The mid-point between the two targets has coordinates (w, h) and the fire is assumed to be fixed at the origin (0,0). Assuming that the two targets are on the line joining the mid-point between them with the origin, the distance between the origin of the fire and the farthest target (r) is given by:

$$r(d,w,h)=\frac{d}{2}+\sqrt{w^2+h^2}$$ [1] (1)

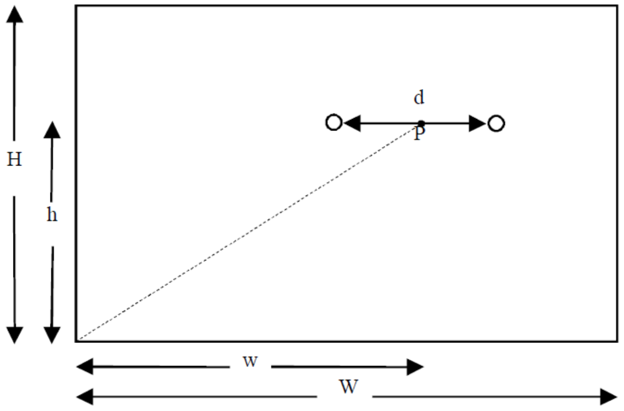

Figure 1: Diagram of MCB Panel with two target elements

The maximum temperature rise above ambient (ΔT) at this distance from the fire is calculated from Alpert's correlation for fire plume temperature:

$$\Delta T=16.9\left[\frac{(kQ)^{2/3}}{r^{5/3}}\right], \quad (2)$$

Where:
k = location factor = 2 for a vertical wall
Q = heat release rate [kW]
r = vertical distance above origin of fire [m]

Applying the plume correlation is clearly pessimistic as, in general, the farthest target will not be in the fire plume, i.e. vertically above the origin of the fire.

The heat release rate (Q) is assumed to follow a t^2 growth rate, rising to its peak value $\hat{Q}$ in 12 minutes. Thus:

$$Q=\begin{cases}\hat{Q}\cdot\left(\frac{t}{12}\right)^2 & t\leq 12\\ \hat{Q} & t>12\end{cases} \quad (3)$$

The rate of decay after reaching the peak heat release rate is immaterial in this methodology, since the temperature rise is assumed to be dependent only on the instantaneous value of the heat release rate (Q) and not on the cumulative quantity of heat released.

The time taken to suppress the fire is modelled as a random variable $(\hat{t})$ with an exponential distribution, i.e.

$$\hat{t}=\frac{1}{t_m}\exp\left(-\frac{t}{t_m}\right), \quad (4)$$

where

t_m = mean suppression time

[1] Although not explored in this paper this approximation itself can introduce errors (e.g. if w is close to zero, and h is a large value, the results will be very inaccurate). A more accurate expression would be $r = \mathrm{sqrt}((w+d/2)^2+h^2)$

To simplify the analysis, all target sets are defined in terms of the distance *d* between the targets corresponding to a calculated *ccdp*. Using this definition, the frequency of damage can be written as a function of *d* as;

$$\lambda (d) = \lambda_{MCB} * [SF \cdot P_{ns}](d) \quad (5)$$ [2]

Where λ_{MCB} is the overall fire frequency of the Main Control Board, *[SF · Pns](d)*, a function of *d*, is the overall likelihood of damage to a target set with maximum internal distance (*d)* among its elements. That is, the likelihood of an unsuppressed fire inside the MCB severe enough to damage the furthest target. Figure L-1 (see figure 2) depicts the final numerical values of *[SF · Pns](d)* as a function of (*d)*.

The full derivation of NUREG/CR 6850, Figure L-1 was not explained in NUREG/CR 6850. However, the derivation has more recently been provided in Draft FAQ -16-00xx [2] and an NEI Task Force White Paper [3] which describes an update of Figure L-1 to account for the new HRRs reported in NUREG 2178 [4] and non-suppression probability reported in NUREG 2169 [5]. During a review of this derivation by Jacobsen Analytics, errors were identified indicating that the solutions reported in both the draft FAQ, as well as in NUREG/CR 6850, are non- conservative and result in a potentially significant under prediction of the fire damage probability. Jacobsen Analytics have subsequently worked in conjunction with Jensen Hughes to explore potential conservative features within the original Appendix L model, which when accounted for were shown to adequately cancel the non-conservative inaccuracies of the model solution. Specifically; the model now uses a reduced plume correlation k factor of 1.0 rather than 2.0 (consistent with the work presented in EPRI TR-3002005303 [6]) and caps the fire peak heat release rate to the 98% percentile of the associated gamma distribution consistent with practice in other areas of detailed fire modelling. Further explanation can be found in the NEI white paper [3] together with the updated Appendix L curves.

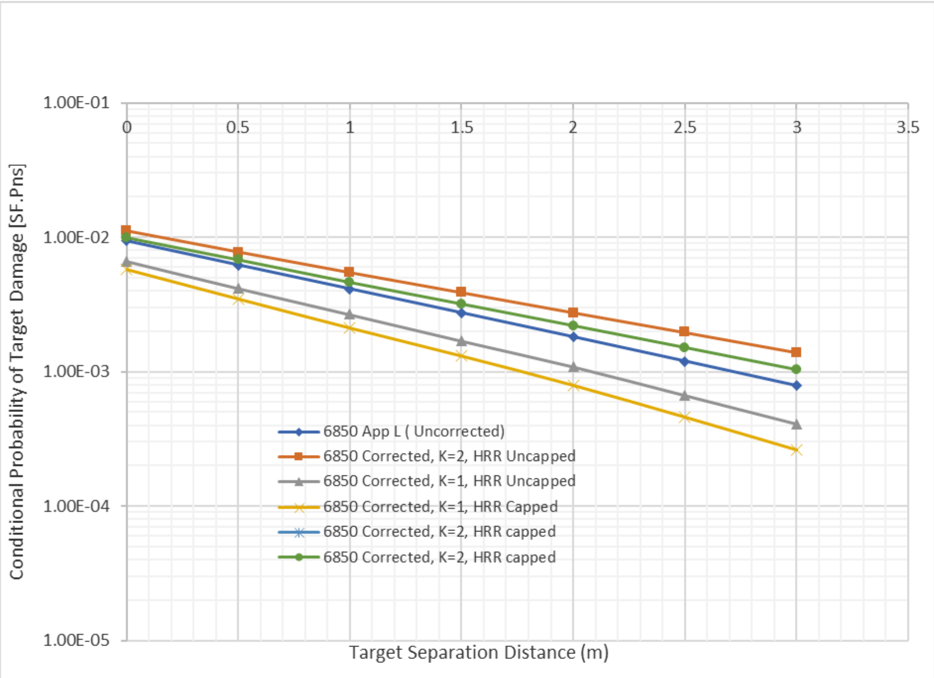

Figure 2: NUREG/CR- 6850 Appendix L compared with Various Corrected Model Results for Thermo Plastic Cable

[2] Equation as written in NUREG/CR 6850 Appendix L

3. MONTE CARLO SIMULATION

The method of solving the Appendix L model proposed in NUREG/CR 6850 and the NEI White Paper relies on the solution of the following expression (3):

$$SF(w,h)\overline{p_{ns}} = 0.02\, p_{ns}(w,h,Q98) + \int_{Q(w,h)}^{Q98} p_{ns}\left(w,h,Q_{peak}\right) f\left(Q_{peak}\right) dQ_{peak} \tag{6}$$

Where: Q_{peak} is the peak heat release rate selected from a gamma distribution, *Q98* is the 98th percentile of that distribution and *Q(w,h)* is the heat release rate required to damage the targets

The solution uses a double integral performed over all allowed values of *w* and *h*, to generate an overall average non-suppression probability across all values of *w* and *h* in the range 0 to *W* and 0 to *H*. A code for this purpose is available for download at http://www2.jacobsen-analytics.com/. However, for those engineers without knowledge of Python coding, a more flexible approach has been developed using Microsoft EXCEL worksheet employing a Monte Carlo simulation add-in, namely Crystal Ball©

In this case the temperature rise (ΔT) at a distance (r) from the origin of the fire for any values of d, w, h and Q is solved using equations (1) and (2). Using the "Crystal Ball" software, a simulation is performed to model the variability of the target location, the peak heat release rate and the time to suppress the fire.

For each iteration the following steps are performed:

1. The location of the mid-point between the two targets is chosen at random assuming that w and h are uniformly distributed between 0 and 60 ft. and between 0 and 10 ft. respectively, assuming the same panel dimensions as Appendix L.
2. The value of (r) is calculated from Eqn. (1) for given value of *d*.
3. The peak heat release rate is chosen at random from a Gamma distribution with shape and scale parameters corresponding to those prescribed for Group 4a cabinets (open/ closed, qualified and non-qualified) in NUREG 2178)
4. The suppression time t is sampled from the exponential distribution (see Eqn. (4)) taking the mean suppression rate of 0.324/min as recommended for control room fires in NUREG-2169 Table 5-1 [5].
5. The heat release rate immediately before the fire is suppressed is calculated from Eqn. (3) using the peak heat release rate sampled at each iteration of the MC solution in step 3, and the corresponding temperature rise at the farthest component from the fire in the target set is calculated from Eqn. (2). (If the suppression time is greater than 12 minutes, the HRR is set equal to the peak value.)
6. If the temperature rise is greater than the damage threshold temperature of 330 °C for qualified cable or 205 °C for unqualified cable, a failure is recorded.
7. The probability of component failure is calculated as the mean number of failures recorded in Step 6, calculated as a fraction of the total number of iterations performed.
8. The calculations are repeated for a large number of iterations until the probability of failure converges to a steady value (typically after a few hundred thousand iterations).

The analysis is then repeated for a range of values of (d) between 0 and 3m.

The Monte-Carlo representation of the Appendix L model within EXCEL/ Crystal Ball is shown in Table 1 for thermo plastic cable in a closed cabinet. The sampled variables (defined as "assumptions" in Crystal Ball terminology) are shown in green. The forecast values (failed =1, not failed = 0) are shown in blue. The results of the Monte Carlo Solution show good agreement with those reported in the NEI White Paper [3] as shown in figure 3.

Run number / Worksheet *	Enclosure Ventilation (Open/ Closed	Fuel Type* (TS/TP Cables)	Alpha	Beta	98th %tile (kW)	HRR capped at 98th% HRR?	NUREG 6850 'k' value
3	Closed	TP	0.52	145	400.44	Yes	1

d (m)	w (m)	h (m)	r (m)	Qp (kW)	t (mins.)	Q (kW)	T (ºC)	Fail?	[SF.Pns]
0	18.288	3.048	18.5402602	216	3.00	13.5	20.74	0	3.42E-03
0.5			18.7902602			13.5	20.72	0	1.76E-03
1			19.0402602			13.5	20.71	0	8.98E-04
1.5			19.2902602			13.5	20.69	0	4.84E-04
2			19.5402602			13.5	20.68	0	2.34E-04
2.5			19.7902602			13.5	20.66	0	1.22E-04
3			20.0402602			13.5	20.65	0	5.00E-05

Table 1: Appendix L Model Represented in Microsoft EXCEL Monte Carlo Simulation

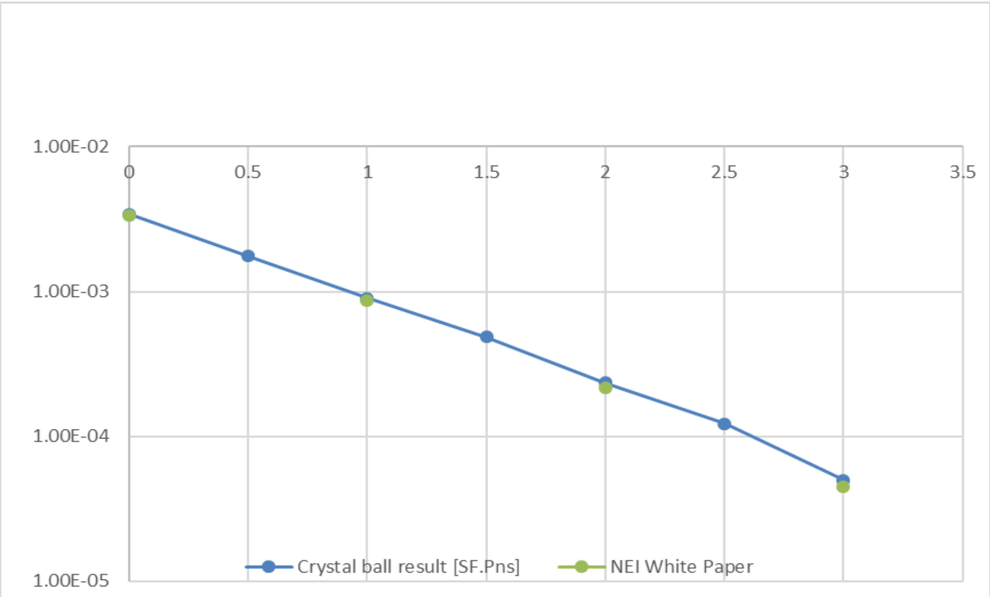

Figure 3: Comparison of Monte Carlo Simulation and NEI White Paper *[SF·Pns](d)* values for Thermo Plastic Cable Closed Cabinet

4. EVALUATION OF APPENDIX L SIMPLIFYING ASSUMPTIONS

This section demonstrates how the Monte-Carlo simulation technique can be used to investigate the sensitivity of the results to the simplifying assumptions made in the analytical method presented in Appendix L and to provide results for a much wider range of situations encountered in practice. The simplifying assumptions made in the Appendix L methodology are identified in the review comments presented below

4.1 Fire and Target Location

To simplify the mathematical analysis in Appendix L, the integration is carried out over all values of the coordinates (w, h) (the mid-point P between the two targets) within the panel boundary. This means that, for values of d greater than zero, the integration will include some positions of the mid-point, near the edges of the panel and remote from the origin, for which the farthest target lies outside the panel boundary. There will also be positions of the mid-point P near the origin (where the fire is assumed to be located) for which the nearest target lies outside the panel boundary allowing the farthest target to be impossibly close to the fire. The overall effect of this edge will be to produce a conservative prediction of the *[SF·Pns](d)* probability with the degree of conservatism increasing with increasing values of *d*.

Another of the most significant limitations of the method used in Appendix L is the assumption that the fire is fixed at the origin, i.e. at one corner of the control panel. This is non-conservative because the distance between the fire and farthest target component is, on average, greater than if the fire were considered to be anywhere else on the panel.

In practice the Appendix L model is applied to specific target sets whose actual position is known within the MCB. Thus, a more appropriate method would perform separate solutions of Appendix L for a variety of fixed individual target midpoint locations (w, h) and target separation distances *d* allowing the position of the fire (x_s, y_s). to vary at random. Figure 4 shows the proposed geometry and Eqn 6 shows the expression used for determining the distance r.

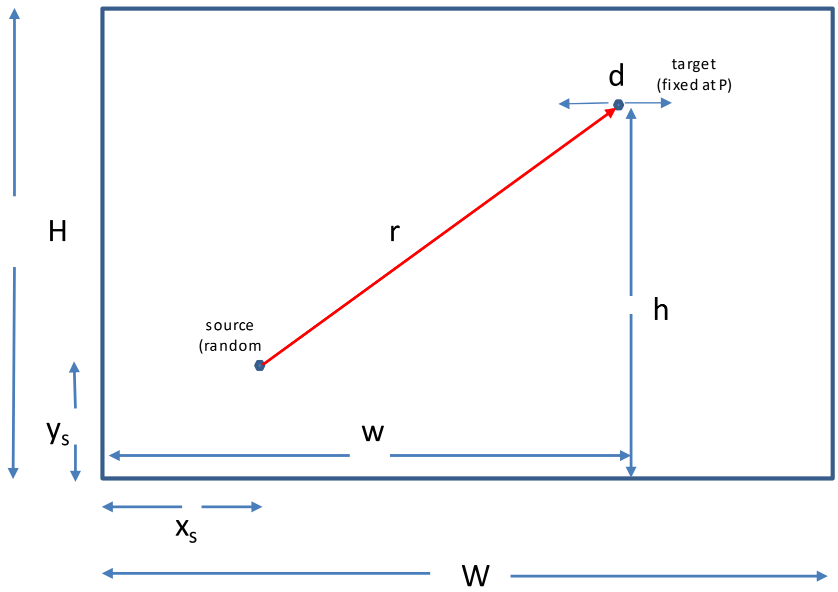

Figure 4: Diagram of MCB Panel with fixed target set and random fire location

$$r(d, w, h, xs, ys) = \frac{d}{2} + \sqrt{((w\text{-}xs)^2 + (h\text{-}ys)^2)} \qquad (7)$$

Figure 5 shows the effect of allowing the fire to be located at random anywhere on a 60 ft. x 10 ft. panel with thermos-plastic cable in an open cabinet as compared with the results from the NEI White Paper (3). These results were obtained using the simulation model described in Section 3 as the basis, with *r* calculated using Eqn 7.

By moving the source randomly this solution generally shows much higher values of [SF*Pns](d) than the NEI white paper (3) except when the target is fixed in bottom left or right corners, which would be expected as the boundary conditions of this solution replicate the NUREG/CR 6850 Appendix L and the NEI Task Force White Paper solution (3)).

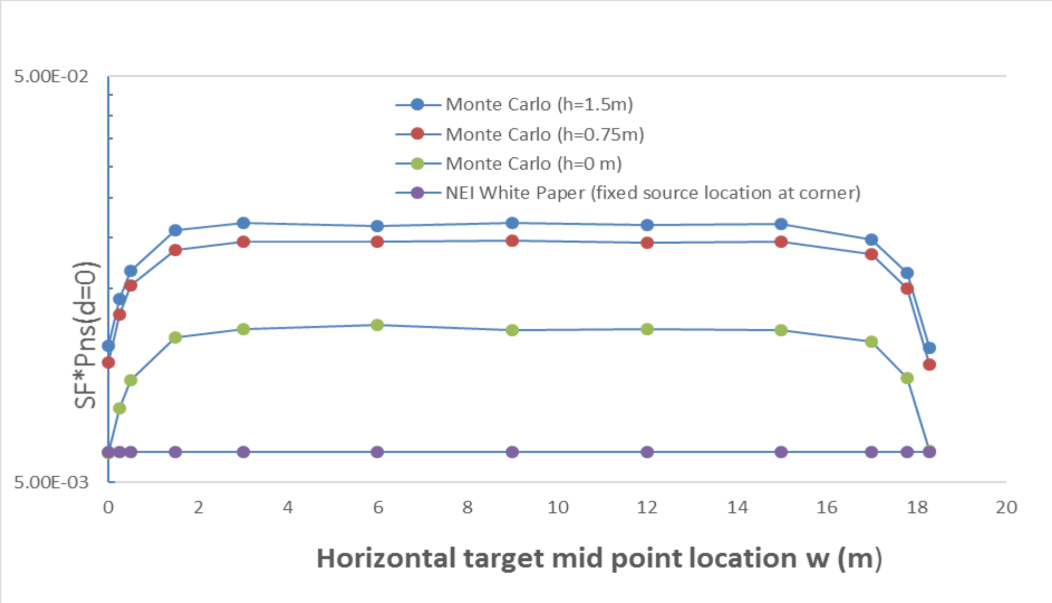

Figure 5: *[SF·Pns] (d= 0)* as a function of target location within MCB vs NEI White Paper Result (3)

4.2 Two Adjacent Cabinets Separated by a Single Wall

For cabinets separated by a single wall with back covers, NUREG/CR 6850 (section 11.5.2.8) permits the analyst to use the approach described in Appendix L to establish the likelihood of fires occurring in the exposing cabinet that could damage the wall. Per the approach recommended in Appendix S, it is assumed that the targets within the exposed cabinet would fail within 15 minutes of a fire impacting the wall between the two cabinets. A second non-suppression probability may be multiplied to the fire scenario frequency based on a 15-minute fire duration (per Appendix S), noted in the equation below:

$$\lambda_{\,Adjacent\ cabinets}(d_a) = \lambda_{\,\mathrm{MCB}}\,[\mathrm{SF}\cdot \mathrm{P}_{ns}]\,(d_a)\,\mathrm{P}_{ns}(15\mathrm{min}) \qquad (8)$$

Where d_a = maximum distance between target elements and the separating wall inside the exposing cabinet.

The 15-minute delay criterion is an attempt to shortcut modelling the temperature rise inside the exposed panel.

However, this simplified approach ignores the dependence of the non suppression probability (P_{ns}) included within two terms $[SF \cdot P_{ns}]$ (d_a) and $P_{ns}(15min)$ within this expression. It further ignores the rue that the minimum credited non suppression probability shall be limited to 1.0E-03.

This dependence can be easily resolved using a Monte Carlo simulation method as illustrated in table 2.

Run number / Worksheet*	Enclosure Ventilation (Open/ Closed Doors)	Fuel Type* (TS/TP Cables)	Alpha	Beta	98th %tile (kW)	HRR capped at 98th% HRR?	NUREG 6850 'k' value
1	Open	TP	0.38	428	1004.77	Yes	1

d (m)	w (m)	h (m)	r (m)	Qp (kW)	ts (mins.)	Qw 15mins prior to suppression	T at barrier 15mins prior to suppression	Fail	[SF.Pns]wb
0	0	0	0	0	2.14	0	20.00	0	1.24E-04
0.5			0.25			0	20.00	0	8.66E-05
1			0.5			0	20.00	0	5.64E-05
1.5			0.75			0	20.00	0	3.62E-05
2			1			0	20.00	0	2.26E-05
2.5			1.25			0	20.00	0	1.52E-05
3			1.5			0	20.00	0	9.00E-06

Table 2: Appendix L Model with a single wall intervening between targets (d=0)

The approach is similar to that described in section 3.1 with the following exceptions. 1) no damage is predicted providing that the suppression time is less than 15 mins, and 2) given the suppression time is > or = 15 minutes, damage to the targets is predicted if the temperature of the barrier exceeds the damage temperature less than 15 mins before the fire is suppressed. This Monte Carlo simulation illustrates that the NUREG/CR 6850 approach significantly under predicts the probability of damage as shown in table 3.

d (m)	Appendix L [SF*Pns](d)	Pns (15)	NUREG/CR 6850 (SF*Pns) * Pns(15)	Monte Carlo Solution accounting for Pns dependency
0	6.03E-03	7.75E-03	4.67E-05	1.24E-04
0.5	3.71E-03	7.75E-03	2.88E-05	8.66E-05
1	2.32E-03	7.75E-03	1.80E-05	5.64E-05
1.5	1.47E-03	7.75E-03	1.14E-05	3.62E-05
2	9.37E-04	7.75E-03	7.26E-06	2.26E-05
2.5	5.86E-04	7.75E-03	4.54E-06	1.52E-05
3	3.67E-04	7.75E-03	2.85E-06	9.00E-06

Table 3: Comparison of NUREG/CR 6850 versus Monte Carlo solution of MCB target damage with intervening single wall

4.3 Application of Monte Carlo Modeling in 3D modeling of Main Control Board

In the example MCB arrangement the cables enter the cabinets via conduits/sleeves passing through the main control room (MCR) floor into vertical cable risers located inside the back at both ends of each cabinet section (Figures 6 & 7). Cables are generally routed from these risers to the corresponding controls via two banks of four cable raceways, which run horizontally along the length of the cabinets aligned in the same vertical plane. Cables connecting to controls and instruments on the MCB fascia emerge at intervals along the length of the horizontal cable raceways. The Appendix L methodology assumes that the distance between target components or cables is determined by the location of the controls and instruments mounted on the front panel of the MCB. The method is not applicable to the cable raceways that run inside the MCB cabinets, since they are not mounted on the panel itself and moreover they are not point targets. FAQ 14-008 (7) alludes to the need to develop a solution for this type of configuration but up to this point no practical approach has been proposed.

An alternate model has thus been developed using MC simulation and applied to such cases. Fire scenarios are assumed to originate within an electrical component located on the control board front surface. As the fire grows, additional components located on the control board fall within the expanding zone of influence of the fire and become damaged. During this phase of the fire's growth the probability of damaging target sets is determined by the maximum separation distance (d) on the control board between any two components within the set according to the approach in Appendix L.

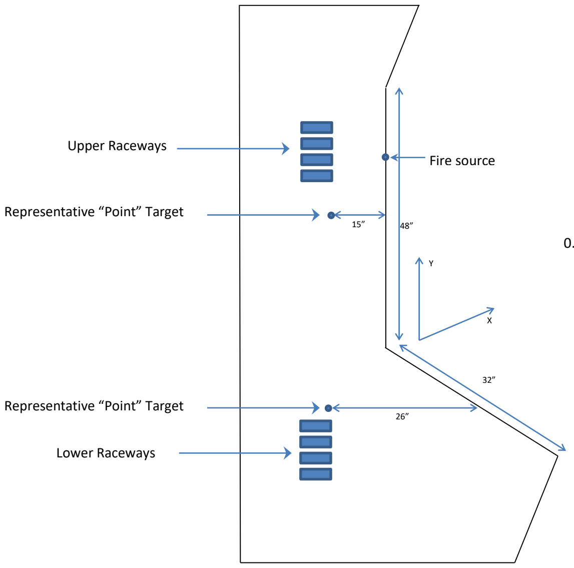

Figure 6: Schematic Section of MCB

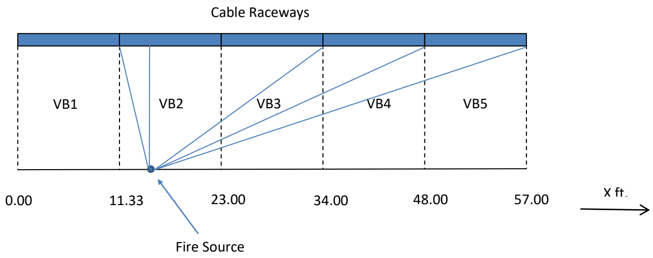

Figure 7: Schematic plan of MCB

However, once the fire achieves a size where its zone of influence encompasses the upper or lower cable raceways located towards the rear of the panel, all components served by those raceways fail. In the case of the upper group of raceways, all components located on the upper section of the board are failed. In the case of the lower raceways, all components on the entire vertical section of the board are failed. This configuration serves to limit the distance over which fire spread on the control board surface is relevant. The MC model also encompasses the possibility of the fire being located in a position where it can impact the raceways of two adjacent sections of the vertical board.

Assuming a radiant heat fraction of 0.4, the heat flux at a distance *r* meters from the fire is then given by:

$$Q_r = \frac{0.4Q_s}{4\pi r^2} \tag{9}$$

The distance *r* is calculated as the closest point to the fire on the section of the cable raceway being considered. If the radiant heat flux exceeds the damage threshold level for a long enough time, cable failure could occur. The relationship between the incident heat flux and time to cable failure is given in Reference 1, Appendix H.

The target is thus assumed to fail if the radiant heat flux exceeds the threshold level (i.e. $Qr > 11$ kw/m2) and the suppression time is greater than the time to failure (i.e. $\hat{t} > td$). To calculate the time to failure it has conservatively been assumed that the cables are exposed to the maximum radiant heat flux throughout the fire growth phase. The upper group of cable raceways were measured as 15" behind the upper, vertical panel of the MCB and, from the geometry of the MCB vertical cabinets, the mean distance between the lower cable raceways and the lower, sloping panel was calculated to be 26". Four separate cases were considered, one each for the upper group of cable raceways affected by a fire on either the upper or the lower panel and one each for the lower cable raceways affected by a fire on either the upper or the lower panel. In each model, the cable raceways were split into five separate sections, corresponding to the five sections of the vertical board (VB1 to VB5) and the probability of a fire anywhere along the whole length of the vertical board damaging any one or more of these sections of the cable raceways was calculated for each of the four cases.

Thus, all scenarios identified using the methodology of NUREG/CR-6850 Appendix L are included in the analysis. If the scenario target set has a value of (*d*) that is less than the corresponding limiting value, the frequency and fire impacts of the scenario are modelled explicitly and if the scenario target set has a value of (*d*) greater than the corresponding limiting value, its frequency and fire impacts are included implicitly within the analysis of the bounding scenario of damage to the cable raceways.

Vertical Board Section(s)	**Upper Cable Raceways**			**Lower Cable Raceways**		
	Fire on upper panel	**Fire on lower panel**	**Fire on either panel**	**Fire on upper panel**	**Fire on lower panel**	**Fire on either panel**
VB1	2.42E-03	6.84E-05	1.48E-03	3.25E-04	7.55E-04	4.97E-04
VB2	2.79E-03	7.44E-05	1.70E-03	3.66E-04	8.91E-04	5.76E-04
VB3	2.67E-03	7.89E-05	1.63E-03	3.33E-04	8.08E-04	5.23E-04
VB4	3.26E-03	9.56E-05	2.00E-03	4.12E-04	9.37E-04	6.22E-04
VB5	1.99E-03	5.52E-05	1.22E-03	2.72E-04	5.96E-04	4.01E-04
VB1,VB2	5.22E-04	1.66E-05	3.20E-04	8.60E-05	1.98E-04	1.31E-04
VB2,VB3	5.31E-04	1.78E-05	3.26E-04	7.70E-05	1.86E-04	1.20E-04
VB3,VB4	5.34E-04	2.12E-05	3.29E-04	7.80E-05	1.63E-04	1.12E-04
VB4,VB5	5.31E-04	1.66E-05	3.25E-04	7.90E-05	1.79E-04	1.19E-04
Fire damaging more than 2 vertical sections negligible	0.00E+00	0.00E+00	0.00E+00	0.00E+00	0.00E+00	0.00E+00

Table 4 Probability of Damage to Cable Raceways within the MCB (Note these results do not include account for the reduced k factor and capped heat release rate described in section 2 as this approach had not been sanctioned at the time the analysis was performed)

Using these values in the scenario frequency calculations for the probability of damage to the target set comprising all the components associated with an individual section of the MCB is conservative. In the above the overall failure probability of the upper or lower cable raceway due to a fire on either the upper or lower panel of a given section of the MCB, was calculated as a mean value, weighted according to the relative frequency of a fire occurring on the upper or lower MCB panel. Assuming that the frequency of a fire on any panel is proportional to the panel area, the weighting factors are 0.6 and 0.4 respectively for the upper and lower panels, which are 48” and 32” in height respectively. Damage probabilities associated with each fire scenario target set are based on the updated NUREG/CR 6850, Appendix L (for scenarios involving component sets located on the MCB board face) and the method described above for MCB cable raceway damage. In either case, the methods used imply the resulting probabilities are not mutually exclusive i.e. they include events involving more widespread damage. Therefore, in order to avoid any double counting of the fire risk which may arise from the summation of the contribution from multiple fire scenarios, mutually exclusive damage probabilities for each fire scenario have been derived. Figure 8 shows an example of the Event Tree approach used for this purpose.

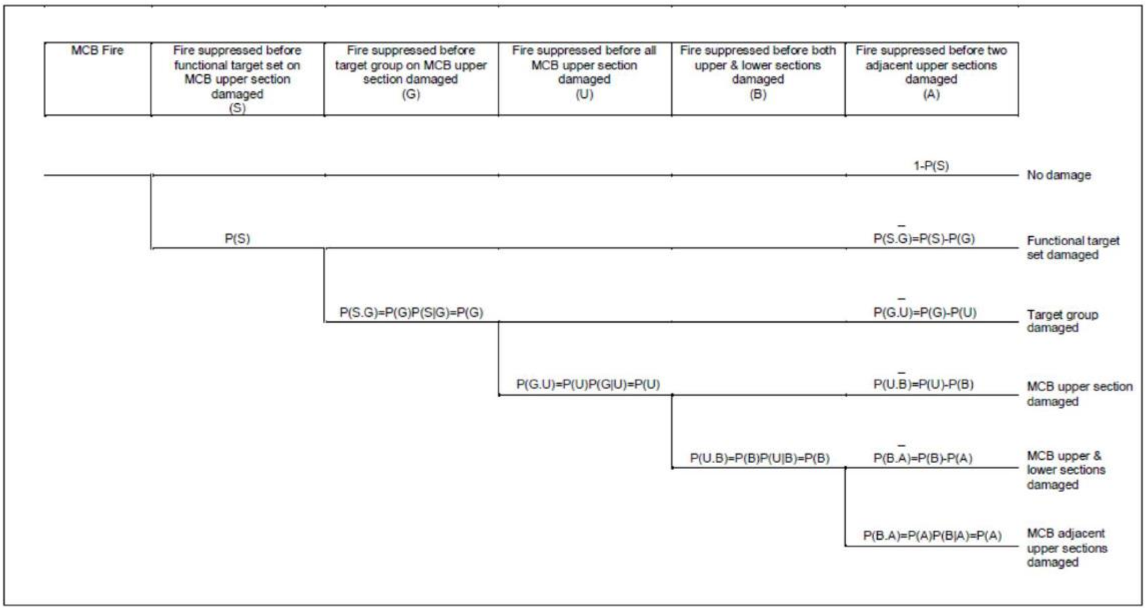

Figure 8: Fire scenario event tree for MCB upper section targets

5.0 CONCLUSIONS

In the absence of an existing verified and validated computational tool to determine the probability of damage to a target set of components due to a MCB fire, a method was proposed in NUREG 6850 Appendix L. However, to simplify the mathematical analysis, a number of assumptions and approximations were made that limit the applicability of the method in practice. A review of these assumptions has been carried out and presented above.

An alternative approach has been taken, using the Monte-Carlo simulation technique, and shown to give results in good agreement with those derived analytically in Appendix L when the same assumptions are made and appropriate corrections were made to the Appendix L analytical solution.

The Monte-Carlo simulation model was then used to investigate the sensitivity of the results to a number of the most restrictive assumptions made in Appendix L, namely:

· Target location defined by mid-point lying within the panel boundary ("edge effect");
· Fire location fixed at origin.
. Evaluation of internal barrier effectiveness

The sensitivity studies show that the overall effect of these assumptions is to potentially underestimate the probability of target damage significantly. Although it is recognised that conservative factors such the likelihood of fire progression beyond the incipient stage and the use axi-symmetric plume model may go some way to compensate for this.

The method has also been extended to consider three dimensional effects of fire that may result from damage to targets away from the control board fascia (as discussed in FAQ 14-0008) and has proposed a practical solution for evaluating the associated risk. This approach also considers targets which are not necessarily located at single points.

The use of Monte-Carlo simulation with Excel spreadsheets enabled with an MC add-on such as Crystal Ball is a user-friendly approach that is a natural extension of a basic spreadsheet model, allowing MC analysis to be accessible without the need for knowledge of highly technical and specialised codes. The studies reported here demonstrate the flexibility of the Monte-Carlo simulation technique in its application to MCB fire analysis. The method can easily be extended to simulate complex 3-D geometries, including the location of sources anywhere in the MCB and the effect of cable routing inside the cabinet which may compromise the spatial separation of components observed on the MCB fascia. More realistic modelling of the effects of fire could also be incorporated to include radiant damage ceiling jet effects and formation of a hot gas layer within an enclosed cabinet. The use of the MC technique also facilitates the propagation of modelling and parameter uncertainties through the fire modelling process.

References

[1] EPRI / NRC-RES Fire PRA Methodology for Nuclear Power Facilities, EPRI TR 1011089 / USNRC NUREG/CR-6850, August 2005.

[2] FAQ 16-00xx: Revised NUREG/CR-6850 Appendix L Figure L-1 using NUREG-2178 heat release rates. Revision A

[3] NEI NFPA 805 Task Force White Paper, “Update of NUREG/CR-6850, Appendix L SF x NSP Curves Incorporating NUREG-2169 and NUREG-2178 data (Revision 1, July 2017)

[4] United States Nuclear Regulatory Commission and Electric Power Research Institute, Refining and Characterizing Heat Release Rates from Electrical Enclosures During Fire (RACHELLE-FIRE), USNRC NUREG-2178 / EPRI TR 3002005578, DRAFT December 2015.

[5] EPRI / NRC-RES United States Nuclear Regulatory Commission and Electric Power Research Institute, Nuclear Power Plant Fire Ignition Frequency and Non-Suppression Probability Estimation Using the Updated Fire Events Database / United States Fire Event Experience Through 2009, USNRC NUREG-2169 / EPRI TR 3002002936, January 2015.

[6] Electric Power Research Institute, Fire Modelling Enhancements for Fire Probabilistic Risk Assessment / Fire Location Factor, Transient Fires and Liquid Spill Release Rate, EPRI TR-3002005303, November 2015.

[7] FAQ 14-008: Main Control Board Treatment Rev 1, June 2014